Modeling and Performance Optimization of a Direct Injection Spark Ignition Engine for the Avoidance of Knocking

Michela Costa, Ugo Sorge, Paolo Sementa and Bianca Maria Vaglieco
Istituto Motori, CNR, Via Marconi, 4, 80125, Naples, Italy

Keywords: CFD Optimization, 3D Engine Model, GDI Spark Ignition Engine, Control, Knocking.

Abstract: The paper applies simulation techniques for the prediction and optimization of the thermo-fluid-dynamic phenomena characterising the energy conversion process in an internal combustion engine. It presents the development and validation of a 3D CFD model for a GDI optically accessible engine operating either under stoichiometric homogeneous charges or under overall lean mixtures. The model validation is realized on the ground of experimental measurements of the in-cylinder pressure cycle and of the available optical images. The model comprehends properly developed sub-models for the spray dynamics and the spray-wall interaction. This last is particularly important due to the nature of the mixture formation mode, being of the wall-guided type. In the stoichiometric mixture case, the possible occurrence of knocking is also considered by means of a sub-model able to reproduce the pre-flame chemical activity. The CFD tool is finally included in a properly formulated optimization problem aimed at minimizing the engine specific fuel consumption with the avoidance of knocking. The optimization, performed through a non-evolutionary algorithm, allows determining the best engine control parameters (spark advance and start of injection).

1 INTRODUCTION

Present work has the primary purpose of showing how a properly developed simulation tool may be of importance for the prediction of the behaviour of a complex system as a gasoline direct injection (GDI) spark ignition engine, hence for the choice of the optimal control parameters of its actual operation.

The well-established role of computational fluid dynamics (CFD) as a tool for the analysis of thermo-fluid-dynamic systems is further confirmed by its application in the design phase of energy conversion systems, and, in particular, of internal combustion engines. Simulation analyses allow running a virtual prototype of a certain propulsion system and testing various geometric configurations or control parameters within time and costs absolutely negligible if compared with the corresponding characterization at the test bench. Just the increasing complexity of modern engines, consequent the large number of parameters that govern their operation, and the need to respond to higher and higher performance targets, may justify the importance of appropriate calculation tools able to describe the relevant phenomenology, especially in the phase of design and prototype development (Carling, 2010).

The use of rigorous methods of decision-making, such as optimization methods, coupled with modern tools of numerical simulation, on the other hand, is today very effective to reduce costs, improve performance and reliability and shorten the time to market of technical systems and components. In fact, numerical procedures may be used to generate a series of progressively improved solutions to the optimization problem, starting from an initial one, until a given convergence criterion is satisfied (Thévenin, 2008). In this perspective, automatic searching methods may strongly reduce the time needed for computational engine optimization effected through parametric analyses.

The state of the art of computational models and optimization methods for internal combustion engine development can be found in the book by Shi, Ge and Reitz (2011): engine optimization through parametric analysis is compared with optimizations realised through non-evolutionary methods or evolutionary methods. Several examples are provided.

In the present paper, the development of a simulation model able to predict both the mixture formation and the combustion processes occurring within the combustion chamber of a high

Costa M., Sorge U., Sementa P. and Vaglieco B..
Modeling and Performance Optimization of a Direct Injection Spark Ignition Engine for the Avoidance of Knocking.
DOI: 10.5220/0005040204840496
In *Proceedings of the 4th International Conference on Simulation and Modeling Methodologies, Technologies and Applications* (SIMULTECH-2014), pages 484-496
ISBN: 978-989-758-038-3

performance GDI engine working under a mixed mode boosting (Alkidas, 2007) is described. The mixed mode boosting consists in a stoichiometric charge operation at high load and a lean charge operation at the lower loads and speeds (Oh and Bae, 2013, Park *et al.*, 2012). The 3D engine model validation, indeed, is shown with reference to both these conditions. The main feature of the engine under study is the optical accessibility to the combustion chamber, which allows also collecting images of the in-cylinder spray evolution and flame development. In a certain relevant operating condition, the possibility of occurrence of abnormal combustions is also analysed, in particular with reference to the phenomenon of spontaneous ignition arising in the so-called end-gas zone, not yet reached by the flame front initiated by the spark plug. The developed simulation tool is finally applied to realize the best choice of the engine governing parameters for the operation with the lower fuel consumption and the avoidance of knocking.

The work description follows the steps described below:

- experimental set-up and campaign;
- development and validation of a 3D model for sprays issuing from new generation high pressure GDI injectors;
- formulation and validation of a 3D model for the simulation of the whole operating cycle of a GDI engine;
- validation of a sub-model for the prediction of the knocking occurrence.
- reduction of the specific fuel consumption and avoidance of knocking under a stioichiometric charge operation.

2 EXPERIMENTAL APPARATUS

The experimental apparatus employed for the collection of data to be used for the validation of the 3D engine model includes the following modules: the spark ignition engine, an electrical dynamometer, the fuel injection line, the data acquisition and control units, the emission measurement system and the optical apparatus.

A GDI, inline 4-cylinder, 4-stroke, displacement of 1750 cm^3, turbocharged, high performance engine is the object of the present study. The engine is equipped either with a Bosch 7-hole injector located between the intake valves and oriented at 70° with respect to the cylinder axis, or with a Magneti Marelli 6-hole injector, mounted in the same way. Mixture formation is realized in the wall guided mode, being the piston head properly shaped to direct the spray and vapour cloud towards the top of the cylinder and the spark plug. The engine is equipped with a variable valve timing (VVT) system in order to optimize the intake and exhaust valves lift under each specific regime of operation. The engine is not equipped with after-treatment devices. Details are reported in Table 1.

Table 1: Characteristics of the engine under study.

Unitary displacement [cm^3]	435.5
Bore [mm]	83
Stroke [mm]	80.5
Air supply	Exhaust gas turbocharger
Max. boost pressure [bar]	2.5
Valve timing	Int. and Exh. VVT
Compression ratio	9.5:1
Max. power [kW]	147.1 @ 5000 rpm
Max. torque [Nm]	320.4 @ 1400 rpm

An electrical dynamometer allows the operation under both motoring and firing conditions, hence detecting the in-cylinder pressure data and exploring the engine behaviour under stationary and simple dynamic conditions.

An optical shaft encoder is used to transmit the crank shaft position to the electronic control unit. The information is in digital pulses, the encoder has two outputs, the first is the top dead centre (TDC) index signal with a resolution of 1 pulse/revolution, and the second is the crank angle degree marker (CDM) 1pulse/0.2degree. Since the engine is 4-stroke, the encoder gives as output two TDC signals per engine cycle. In order to determine the right crank shaft position, one pulse is suppressed via the dedicated software.

A quartz pressure transducer is installed into the spark plug to measure the in-cylinder pressure with a sensitivity of 19 pC/bar and a natural frequency of 130 kHz. Thanks to its characteristics, a good resolution at high engine speed is obtained. The in-cylinder pressure, the rate of heat release and the related parameters are evaluated on an individual cycle basis and/or averaged over 300 cycles.

The tests presented in this paper are carried out at the engine speed of 1500 rpm. The absolute intake air pressure remains constant at 1300 mbar, the temperature is 323 K. Two operating conditions are considered for the 3D model validation, whose control parameters are summarised in Table 2. The first, hereafter indicated with the letter L, is characterized by an overall lean charge; the second

one has a stoichiometric charge, and is indicated with letter S. Start of injection (SOI) and start of spark (SOS) are expressed in crank angles before the top dead centre (BTDC). The injection pressure is equal to 6 MPa in the lean case, to 15 MPA in the stoichiometric case. Commercial gasoline is delivered through the 7-hole Bosch injector. Intake valve opening (IVO), intake valve closing (IC), exhaust valve opening (EVO) and exhaust valve closing (EVC) are all reported in the table caption after (A) or before (B) the relevant dead centre (TDC or bottom dead centre, BDC).

Table 2: Operating conditions considered for the 3D model validation. IVO@13°ATDC, IVC@52° ABDC, EVO@20° BBDC, EVC@15° BTDC.

	SOI [°BTDC]	SOS [°BTDC]	A/F	p_{inj} [MPa]
Overall lean charge (L)	70	13	21.5	6
Stoichiometric charge (S)	307	19	14.7	15

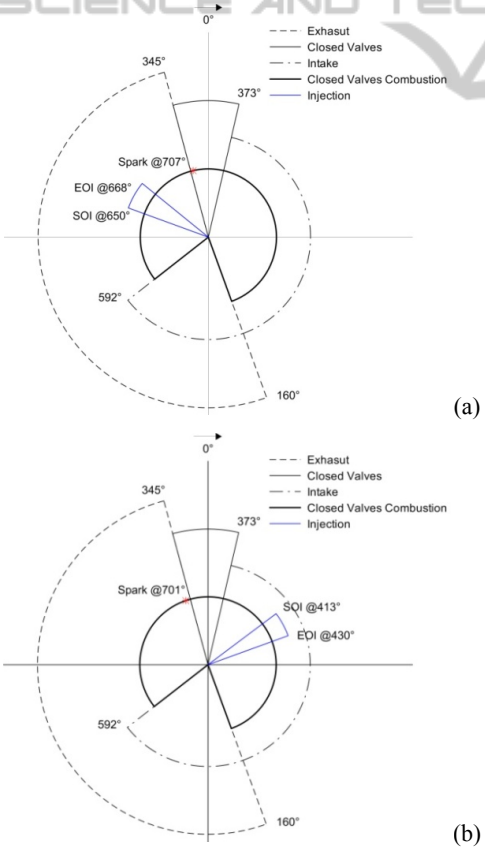

Figure 1: Polar diagrams for the (a) lean burn and (b) stoichiometric case of validation.

The polar diagrams of Figure 1 summarises the synchronization of injection, ignition and valve timing for the cases L and S. The injection occurs entirely during the intake stroke in the S case, entirely in the compression stroke in the L case. Their length is comparable, although the delivered fuel amount is greater in the S case, due to the different injection pressure.

Three different operating conditions are instead employed with the aim of studying the knocking occurrence in the engine under study. The 92 RON fuel is here delivered through the Magneti Marelli 6-hole injector, with governing parameters as reported in Table 3. Figure 2 shows the in-cylinder pressure in the cases of Table 3. In particular, Figure 2a reports the average over 300 consecutive cycles in a no-knocking situation, Figure 2b and 2c represents the instantaneous pressure curves corresponding to the 150th cycle of 300 consecutive ones in an incipient knocking case and a knocking case, respectively. In Figure 2b and 2c the pressure traces show the typical ripples of knock, whose intensity increases as the spark advance is increased.

Table 3: Operating conditions considered for study of the knocking occurrence. IVO@22° BTDC, IVC@17°ABDC, EVO@5° BBDC, EVC@TDC.

	SOI [°BTDC]	SOS [°BTDC]	A/F	p_{inj} [MPa]
No knocking case	200	20	14.7	10
Incipient knocking case	200	25	14.7	10
Knocking case	200	30	14.7	10

2.1 Optical Apparatus

The engine under study is optically accessible. Imaging measurements are performed by means of the optical experimental set-up shown in Figure 3. The optical accesses are realized in the engine head, as reported in Figure 3.b. A customised protective case for an endoscopic probe, equipped with an optical sapphire window (5 mm diameter), is installed in the engine head in the 4th cylinder. This system allows investigating an area including the spark and the gasoline spray through an endoscope exhibiting a viewing angle of 70°. The field of view is centred in the combustion chamber perpendicularly to the plane identified by the axes of the cylinder and the injector, hence perpendicular to the plane of tumble motion. The endoscopic probe is coupled with two high spatial and temporal resolution CCD cameras. The first is an intensified

cooled CCD camera (ICCD). It is equipped with a 78 mm focal length, f/3.8 UV Nikon objective.

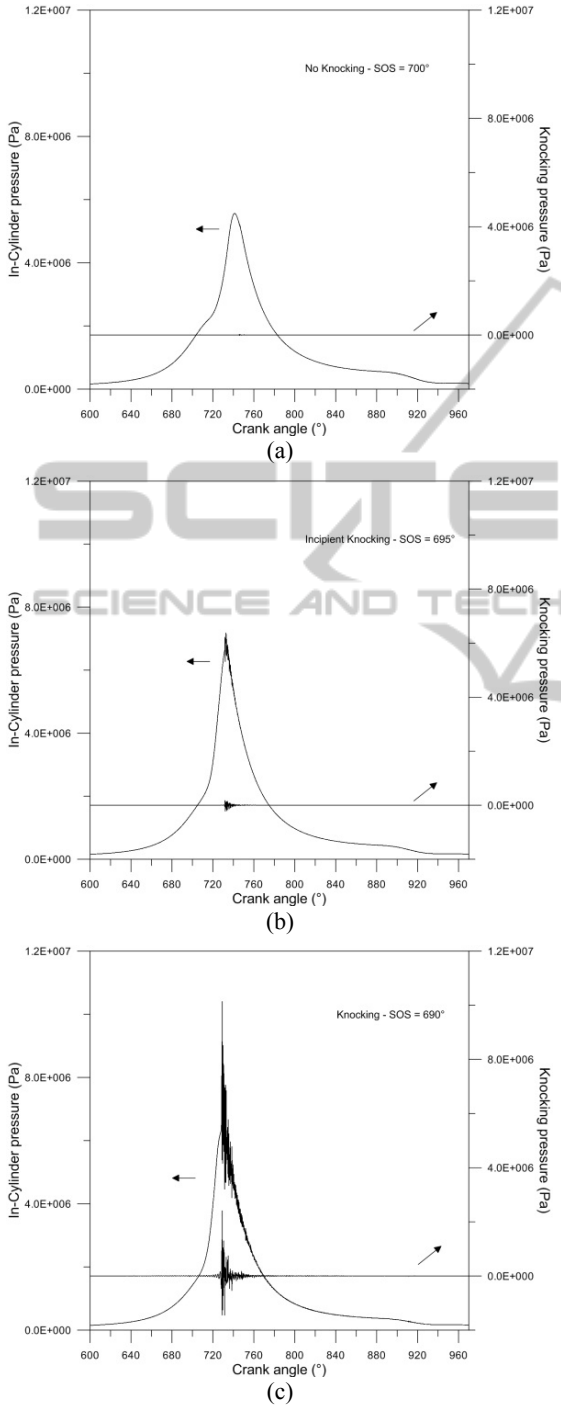

Figure 2: In-cylinder pressure in the (a) no knocking, (b) incipient knocking and (c) knocking case and 5-30 kHz band pass filter.

The ICCD has an array size of 512x512 pixels and a 16-bit dynamic range digitization at 100 kHz. The optical apparatus allows a spatial resolution of approximately 0.19 mm/pixel. Its spectral range spreads from UV (180 nm) until visible (700 nm).

The ICCD operates at a digitizer offset of about 230 counts, but the dark noise fluctuation in the background is much smaller, less than 50 counts. Dark noise and photon statistical noise are both small compared with the measured intensity. The second camera is a digital CCD colour camera equipped with a 50 mm focal length, f/3.8 Nikon lens (Figure 3.a). Its spectral range spreads from 400 to 700 nm and it allows performing a 2D flame visualization. The spatial resolution for this other optical assessment is of about 0.19 mm/pixel.

The gasoline injection phase is characterized through the ICCD camera and an intense strobe lamp, which is introduced in the spark location through a fiberoptics. For all the optical measurements, the synchronization between the cameras and the engine is made by the crank angle encoder signal through a unit delay.

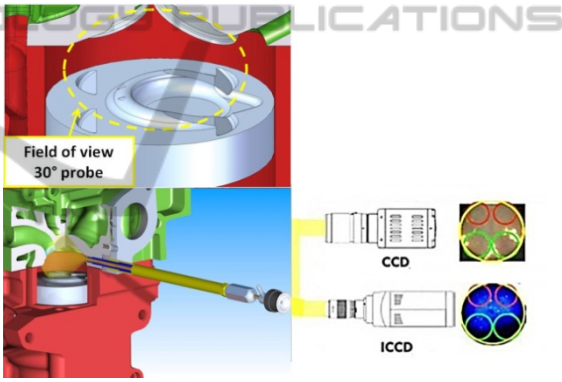

Figure 3: Sketch of the experimental setup for optical investigation and detail of the combustion chamber: a) CCD for 2D two colour technique, b) ICCD for UV-Visible acquisition.

3 SPRAY SIMULATION

The analysis of the models available in the literature for the simulation of sprays generated by new generation GDI injectors, carried out in order to identify any inadequacies and issues for potential improvement, has highlighted the need for the development of a sub-model suitable of being used in different operating conditions of a modern GDI engine. In fact, already in the GDI exclusive operation with homogeneous charges, namely in what could be called the first generation GDI engines, a crucial role was played by the interaction between the spray of injected fuel and the air

turbulent motion within the combustion chamber. The complex phenomena of penetration, transport and evaporation of gasoline had to be carefully controlled in order to allow the desired homogeneous preparation of the mixture and the minimization of anomalies such as the presence of liquid particles on the walls or any localized thickening of fuel deposits (Stan, 2000, Zhao, 2001). In the new generation GDI engines, based on the so-called mixed mode boosting, the concentration of fuel vapor in the combustion chamber may be differentiated at the medium loads in order to create a zone with air-fuel ratio stoichiometric or slightly rich in the vicinity of the spark plug, and lean in the vicinity of the cylinder walls. Globally, the mixture ratio can be lean (lean burn). At higher loads, and at all loads and higher speeds, the engine may be operated in a stoichiometric homogeneous mode. The control of the formation process of the air-fuel mixture, therefore, is an objective of great interest, as detrimental in ensuring flame stability, reduction of produced pollutants and high combustion efficiency.

The 3D sub-model able to simulate the dynamics of the gasoline spray issuing from the considered injector is here developed in the context of the software AVL Fire^{TM}, in such a way to simulate preliminary experiments performed by mounting the injector and delivering sprays in an optically accessible vessel. The followed approach is the classical coupling between the Eulerian description of the gaseous phase and the Lagrangian description of the liquid phase. The governing equations are here not reported for the sake of brevity; the interested reader may refer to the book by Ramos (Ramos, 1989). The train of droplets inserted in the computational domain in correspondence of the injector holes exit section suffers various concurring effects as it travels. Details of the model are given in the paper by Costa *et al.* (2012). Here it is only worth pointing out that the droplets break-up phenomenon is simulated according to the sub-model of Huh-Gosman (1991), whose constant C_1 (regulating the break-up time) is adjusted in a tuning procedure. The effects of the turbulent dispersion on the droplets dynamics is simulated through the sub-model by O'Rouke (O'Rouke and Bracco 1980), the coalescence through the sub-model by Nordin (2001), the evaporation through the sub-model by Dukowicz (1979).

Initial size of droplets at the nozzle exit section, is considered as variable according to a probabilistic log-normal distribution, whose expected value is given by the following theoretical diameter, where τ_f is the gasoline surface tension, ρ_g the surrounding gas density, u_{rel} the relative velocity between the fuel and the gas, C_d a constant of the order of the unity (indeed taken equal to the unity), and the parameter λ^* deriving from the hydrodynamic stability analysis and indicating the dimensionless wavelength of the more unstable perturbation to the liquid-gas interface at the injector exit section:

$$D_{th} = C_d \left(\frac{2\pi\tau_f}{\rho_g u_{rel}^2} \right) \lambda^* \qquad (1)$$

The variance of the distribution, σ, is another sub-model parameter to be properly tuned.

The model tuning is effected through an automatic procedure developed by authors, that solves a single objective optimization problem. In other words, instead of resorting to a search of the values of the constants by trial and error, i.e. for successive approximations, an optimization problem is set-up, where the Nelder - Mead Simplex algorithm (Nelder and Mead, 1965) is used to reduce the error between the results of the numerical computations and the experimental measurements relevant to the penetration length. The automatic procedure allows obtaining a model of high "portability", i.e. such to be applied as it is to different operating conditions, or even to sprays generated by different injectors.

The tuning procedure is hereafter described. Experimental tests are reproduced by simulating the spray dynamics within a domain reproducing in size and shape the used confined vessel. At each injection pressure, the log-normal distribution of the initial droplet size at the injector exit section is built starting from the value of σ chosen in the design of experiments (DOE) space and the value of the expected value computed according to eq. (1). The distribution profile is transferred to the Fire^{TM} spray sub-model, that also receives the value of C_1 from the DOE space. The model performs the spray computation in the interval of time needed to inject a given mass of gasoline (according to the experimental measurements), and furnishes, as an output, the penetration length of the jets compounding the spray. The error between the numerically computed penetration length, as averaged over the six (or seven) jets, and the experimentally measured one is minimized by the Simplex algorithm. The objective function is defined as :

$$Obj\big|_{\sigma,C_1} = \sum_{i=1}^{n} \left[l_{ex}(t_i) - l_{num}(t_i) \right]^2 , \qquad (2)$$

where n represents the number of discrete instants of time in which the injection interval of time is subdivided, t_i is the i^{th} instant of time, and $l_{ex}(t_i)$ and $l_{num}(t_i)$ the values, respectively, of the experimentally measured and the numerically computed penetration length at t_i. The experimentally measured penetration length, indeed, is evaluated by means of a smoothing spline passing through the actual measurements points in the time-length plane.

Some results of the developed spray sub-model, in its application to the 7-hole Bosch injector, are summarised in Figure 4, where the comparison between the experimentally measured penetration length (of one of the seven jets compounding the spray) and the numerically computed one (as averaged over the seven jets) is reported for two different injection pressures.

The prediction capability of the sub-model is demonstrated by the really satisfactory agreement between numerical and experimental data under all the injection pressures.

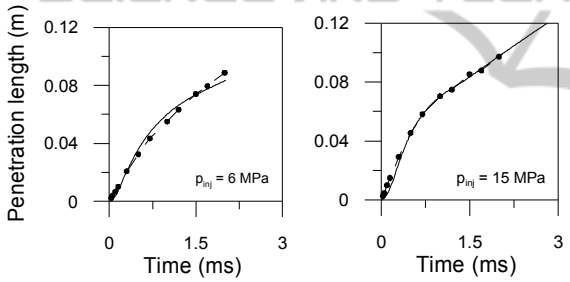

Figure 4: Numerical (continuous line) and experimental (dashed line with dots) penetration lengths of the GDI spray in a confined vessel at various injection pressures.

Moreover, the developed model also proves being satisfactory in its application to the Magneti Marelli 6-hole injector, as demonstrated in the paper by Costa *et al.* (2014).

As previously mentioned, in the considered engine, mixture formation occurs in a wall guided mode, with the spray directed towards a properly shaped cavity on the piston head, which makes for the spray droplets and vapour cloud to move in the proximity of the spark plug. The spray wall impingement, therefore, plays a fundamental role. This is the reason why particular care is devoted to account for the phenomena consequent the impact, namely the droplets fragmentation, sticking, rebound and evaporation as a consequence of the heat transferred from the hot piston wall to the droplets, which contributes to the latent heat of vaporization. The sub-model proposed by Kuhnke (2004) is preferred to the one by Mundo *et al.* (1995).

4 3D ENGINE MODEL

The formulation of the 3D engine model is carried out within the AVL Fire™ environment, although the choice of the software is not binding. As previously mentioned, the simulation model of the working cycle of the GDI engine object of study is based on the coupling between the balance equations of mass, momentum and energy for the gaseous phase, written according to the Eulerian approach, and the Lagrangian treatment of the liquid phase. The mass of gasoline that at each crank angle undergoes the phase change from liquid to vapor, in each computational cell, constitutes a source term for the mass balance equation of the gas phase. The whole 4-stroke cycle is simulated. Boundary conditions for the 3D model are obtained from test bench data.

The discretization of the computational domain corresponding to the cylinder and the intake and exhaust ducts of the considered engine is made through the pre-processing module Fame Engine Plus (FEP) of the AVL Fire™ code, with part of the domain discretized "manually" to increase the mesh regularity and assure stability of computations.

Figure 5 shows a computational grid relevant to the closed valve period, where one may note the care devoted in the discretisation of the zone surrounding the spark plug. The nose in the piston head is also visible on the bottom left of the figure, in opposite position to the injector location, that is on the right.

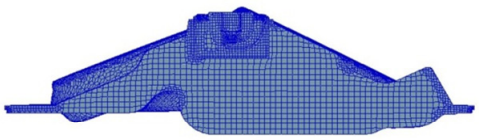

Figure 5: Computational grid at TDC.

The combustion process in the developed engine model is simulated through the Extended Coherent Flamelet Model (ECFM) (Colin *et al.*, 2003), NO formation follows the Zeldovich's mechanism (Zeldovich *et al.*, 1947). The ECFM model is properly tuned to well catch the in-cylinder pressure curve by acting on the initial flame surface density and the flame stretch factor. The validation consisted in a preliminary verification of the results independency upon the grid size, as well as in the calculation of the motored cycle. For the sake of

brevity, further details of the validation procedure of the 3D model are here not reported.

The interested reader may refer to the paper by Allocca *et al.* (2012).

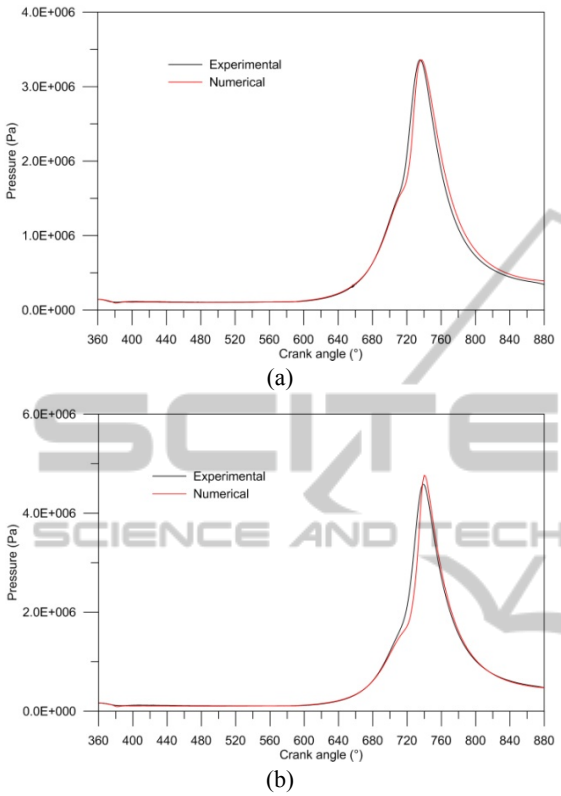

Figure 6: Numerical-experimental comparison between the in-cylinder pressure under (a) lean burn and (b) in the stoichiometric case.

Figure 6.a shows the comparison between the measured pressure cycle (averaged over 300 consecutive cycles) and the cycle calculated numerically in the lean burn case of Table 2. The injection begins 70° BTDC and has duration of 18°; SOS takes place 13° BTDC. Figure 6.b represents the comparison between the calculated and the measured pressure cycles in the stoichiometric case of Table 2. In both the situations the numerical-experimental agreement is really satisfactory.

The different characteristics of the mixture formation process in the two considered cases L and S are well highlighted in Figure 7, where the equivalence ratio distribution of the charge on a plane passing through the spark plug is drawn at the time of spark ignition. The mixture inhomogeneity of the case L is determined by the late injection. In the stoichiometric case, the early supply of gasoline leaves enough time to the perfect mixing of vapour with the surrounding air. The charge stratification of the L case is not optimal, since a rich zone appears on the piston head, in correspondence of the nose.

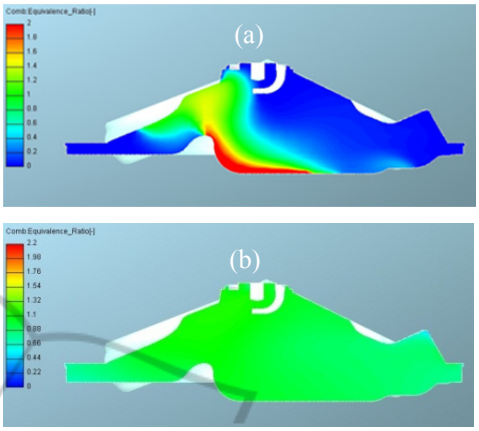

Figure 7: In-chamber equivalence ratio on a plane passing through the spark plug at SOS: (a) case L; (b) case S.

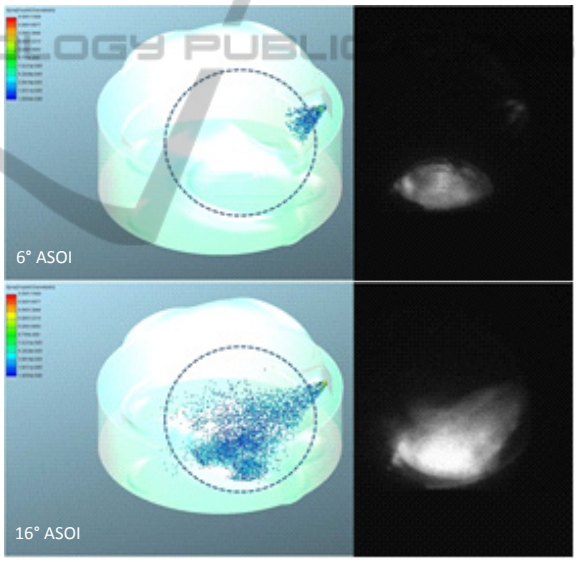

Figure 8: Comparison between numerically computed (left) and experimentally collected images of the spray (right) at two crank angles ASOI, for the Case S.

Information concerning the spray evolution within the combustion chamber can be deduced from Figure 8, where the numerically computed spray and the experimentally collected images are represented for two crank angles after SOI in the S case. The developed numerical model well reproduces the droplet dynamics and impingement on the piston wall, which is moving towards the TDC.

Further confirmation of the good predictive capability of the numerical model is given by Figure 9, which represents the propagation of the flame

front in the stoichiometric mixture in the times immediately following the initiation of combustion, a comparison made possible due to the optical accessibility of the engine under study. In particular, three different angular positions after the ignition are considered. It must be kept into account that the experimental image represents the flame as averaged over the optical path, while the numerical image represents the flame surface density on a plane passing through the spark plug. The slight shift of the flame toward the exhaust valves, on the left side of the figure, is well reproduced numerically.

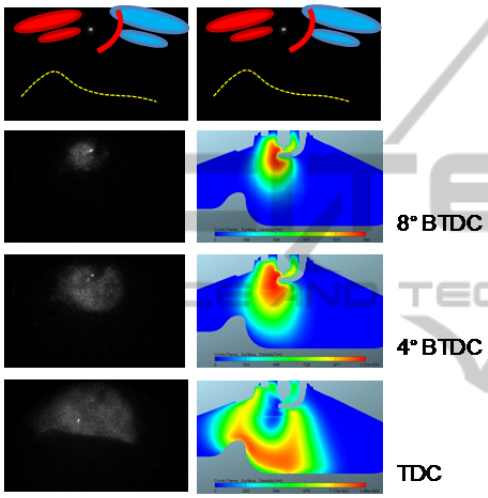

Figure 9: Flame front in the stoichiometric case: experimental (left) and numerical (right) at various times.

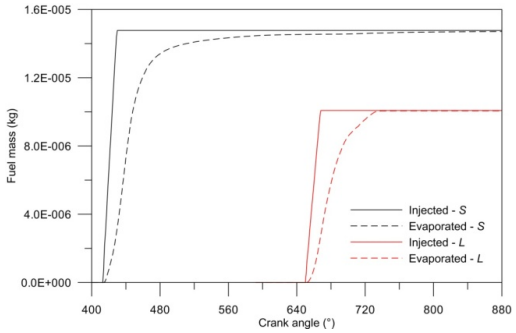

Figure 10: Injected and evaporated gasoline mass in cases L and S.

As an example of the type of results suitable of being obtained through the developed numerical model, one may look at Figure 10, where the trends of the mass of fuel injected and of the mass of fuel evaporated are reported in the two conditions S and L. The evaporation in the case L is not complete at the crank angle of spark advance, and continues during combustion, being enhanced by the

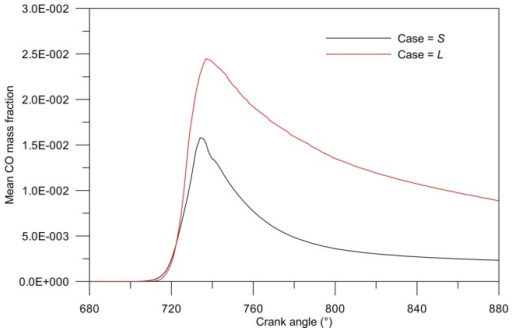

Figure 11: CO mass fraction in cases L and S.

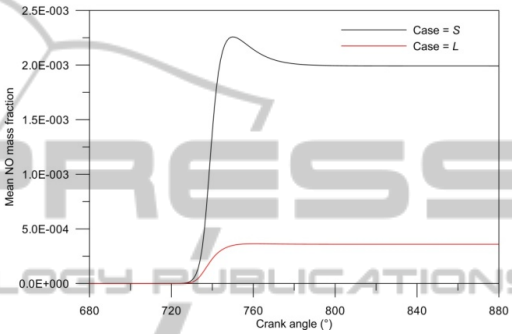

Figure 12: NO mass fraction in cases L and S.

consequent increase of the in-chamber temperature. The production of the main pollutants can instead be discussed with reference to Figure 11 and 12. A greater production of carbon monoxide is observed in the case L due to the incomplete combustion process. Reduced NO amount are evident, due to the lower combustion temperature. Definitely, the here considered lean burn case cannot be considered optimal, but is susceptible of improvement through a different choice of the injection strategy or spark advance.

5 KNOCKING PREDICTION

The study of operating conditions for which abnormal combustions occur is carried out with reference to the knocking phenomenon, namely to situations in which a part of the mixture, before being invested by the flame front ignited by the spark plug reaches conditions that promote its spontaneous ignition. The self-ignition of a fuel-air mixture is the result of a series of pre-flame or low temperature reactions, which lead to the start of the combustion process without the intervention of an external source of ignition, but through the formation of not stable products of partial oxidation (peroxides, aldehydes, hydroperoxides, etc.) and the

release of thermal energy. When the energy of the exothermal chemical reactions exceeds the amount of heat transferred from the reagent system to the external environment, self-ignition takes place. As a result, the temperature of the mixture increases, rapidly accelerating the subsequent oxidation reactions. The speed of the pre-flame reactions, of chain type between highly reactive compounds, can be reduced through the introduction in the fuels of small quantities of additives, which hinder the formation of radicals acting as chain propagators (Leppard, 1991, Li *et al.*, 1994).

The simulation of the process of self-ignition of an air fuel mixture can be performed at different levels of approximation. A model that has proved being successful in predicting both spatially and temporally the occurrence of self-ignition, and that, at the same time, does not require excessive computational time, is the so-called Shell model, developed by Halstead *et al.* (1977). It comprehends the start of combustion, with the break-up of the carbon-hydrogen bond and its development through the formation of oxygenated products.

The main advantages deriving from the use of a reduced scheme with respect to what could be a detailed kinetic scheme, consist precisely in the identification of groups of radicals or radicals that lead to the branching of the reaction chains or to simple propagation of linear type, and in the possibility to follow the variation in time of the concentration of these radicals. Other kinetic mechanisms developed subsequently to the Shell, have a number of reactions and species involved much higher, which makes of little interest their use within numerical simulations on multidimensional complex domains (Griffiths *et al.*, 1994).

The Shell model is here used in the so-called end-gas zone, namely in the volume of mixture not yet reached by the flame front. The combustion process resulting from the spark ignition is calculated using a flamelet model, as already pointed out in the previous paragraph.

Introducing the hydrocarbon RH, namely the fuel of composition CxHy, the Shell model is constituted by the following chemical reactions:

primary initialization

$$RH + O_2 \rightarrow 2R*$$

pre-flame propagation

$$R* \rightarrow R* + P$$
$$R* \rightarrow R* + B$$
$$R* \rightarrow R* + Q$$
$$R* + Q \rightarrow R* + B$$

branching

$$B \rightarrow 2R*$$

linear and quadratic termination

$$R* \rightarrow NR$$
$$2R* \rightarrow NR$$

where the letter P indicates the reaction products (CO_2, H_2O), B and Q, respectively, represent branching agents and generic intermediate species. With the term NR are indicated not reacting compounds created at the end of the pre-flame reactions.

Into detail, the model contemplates the start of combustion, with the breaking of the chains of carbon-hydrogen fuel and the formation of radicals R*, and its development through the formation of oxygenated products. As already mentioned, the species that have a similar role in the pre-flame kinetics are treated uniquely, as if they were a single entity.

The numerical 3D model is first adapted to reproduce the no knocking condition of Figure 2.a, then the spark advance is increased twice, each of 5° crank angle, according to Table 3.

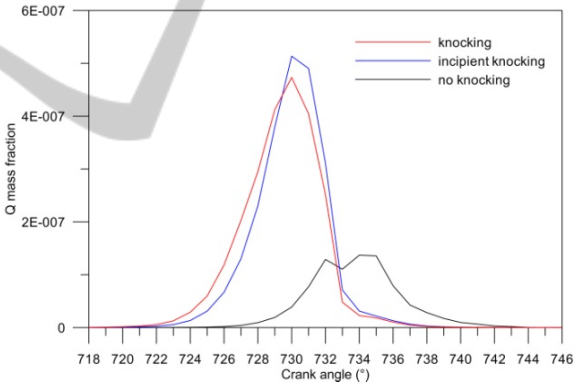

Figure 13: Q formation in the combustion chamber in the three cases of Table 3.

Figure 13 shows the in-chamber formation of Q for the three considered cases and well highlights that with more advanced ignition a more rapid formation of this group of species occurs. The location of the maximum value of the Q concentration at the crank angle of 729° (9° after top dead center, ATDC) is in excellent agreement with the experimental data of Figure 2, in particular with the start of oscillations of the knocking case of Figure 2.c. The Shell model also allows drawing the distribution of the intermediate Q in the combustion chamber, that may help in highlighting the zone where the knocking occurrence is the most probable. Figure 14 represents, in the three situations of Table 3, the

distribution of Q on a plane perpendicular to the cylinder axis (the one at which the maximum mass fraction of the species Q is attained) at the crank angle of knocking occurrence, namely 729°. Due to the symmetry assumption, only half plane is plotted. One may note the greater chemical reactivity in the area of the end-gas located at the bottom of the figure, on the side where injector is mounted.

The shaped nose on the piston head, in fact, appears clearly in the figure. The species Q, therefore, can be used as an index of probability of knocking occurrence. The Shell model, therefore, allows both the spatial and temporal localization of the phenomenon of self-ignition in the end-gas zone.

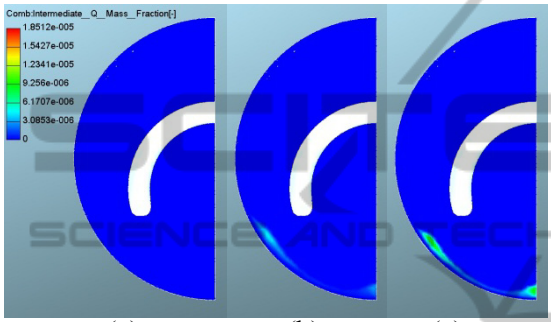

Figure 14: Spatial distribution of the intermediate species of the pre-flame reactions on the plane orthogonal to the cylinder axis of maximum concentration 9° after TDC for the (a) no knocking, (b) incipient knocking and (c) knocking case.

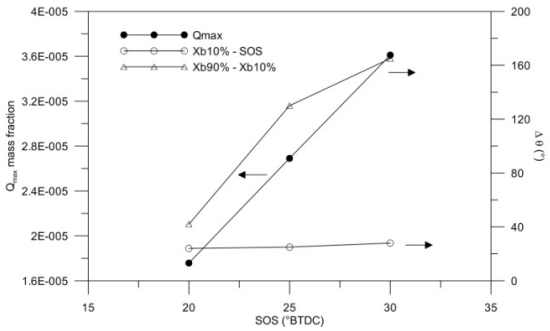

Figure 15: Maximum local value of species Q, flame initiation angle and flame development angle a function of SOS.

Finally, Figure 15 represents the maximum local value of the Q mass fraction as a function of SOS, together with the angles measuring the interval of flame initiation and flame propagation. These may be quantified by the interval of crank angle comprised between SOS and $\theta_{10\%}$ and the interval between $\theta_{10\%}$ and $\theta_{90\%}$, respectively. $\theta_{10\%}$ is the crank angle where the 10% of the mixture is burnt, while $\theta_{90\%}$ is the crank angle where the 90% of the mixture is burnt. It is clear that by increasing the spark advance both the flame initiation and the flame propagation get slower. The greatest intervals needed for flame initiation and development at the highest spark advance, hence the unfavourable conditions of temperature and pressure at spark timing, give the mixture enough time to self-ignite in the end-gas zone.

Based on the afore described calculations and on the analysis of experimental data, one may define criteria for knocking occurrence, either based on the evaluation of the in-cylinder amount of the Q species, or on the more traditional evaluation of the pressure gradient in the p-θ (pressure-crank angle) plane, where a threshold value can be established below which the engine operates regularly (Heywood, 1988). By following this second route, and in agreement with the experimental data, the value of $dp/d\theta=3.5$ was fixed as threshold for the knocking occurrence.

6 ENGINE OPTIMIZATION

Although GDI engine are characterised by lower in-cylinder temperatures with respect to port fuel injection (PFI) engines, knocking occurrence remains an important issue, especially in approaching the design of a new engine prototype and with the aim of defining the control parameters leading to the best engine performance.

A method is here proposed to explore the DOE space of the engine control variables, based on the coupling between the CFD engine model and an optimization algorithm able to point out the condition of maximum power output (the objective function is the maximum integral of pressure in the pressure-volume plane in the closed valve period) and simultaneously avoid the occurrence of the knocking phenomenon. The start of injection (SOI) and start of spark (SOS) are the input parameters of the formulated optimization problem, whose flow chart is represented in Figure 16.

A proper DOE space defines the acceptable limits of these variables. The engine speed, air-to-fuel ratio and valve timing are kept constant. The optimization algorithm, here chosen as the Simplex, runs the 3D engine model towards the optimal solution. Computed pressure cycles that do not satisfy the imposed constraint on the pressure derivative, defined at the end of paragraph 5, are discharged from the optimization results. This

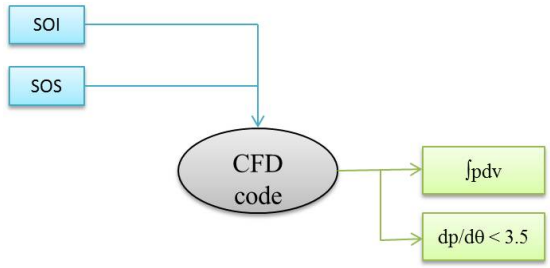

Figure 16: Flow chart of the optimization problem.

approach is preferred to the use of the previously presented Shell model in the 3D code, in order to avoid an excessive increase of the computational time to limits unreasonable for an optimization process.

Table 4: Cases computed with the optimization tool at different SOI and SOS imposed and corresponding $dp/d\theta_{max}$ values.

Id	SOI [°BTDC]	SOS [°BTDC]	$dp/d\theta_{max}$	∫pdv
2	126	40	8.08	272.40
9	122	12	5.38	277.59
15	130	12	3.31	274.44

The obtained results exhibiting the highest value of the objective function are presented in Table 4 and in Figure 17.

Table 4 summarises the value of the input variables SOI and SOS, the objective function and the maximum value of the pressure derivative in the p-θ plane, evaluated in the interval of crank angles ranging between SOS and 10° ATDC.

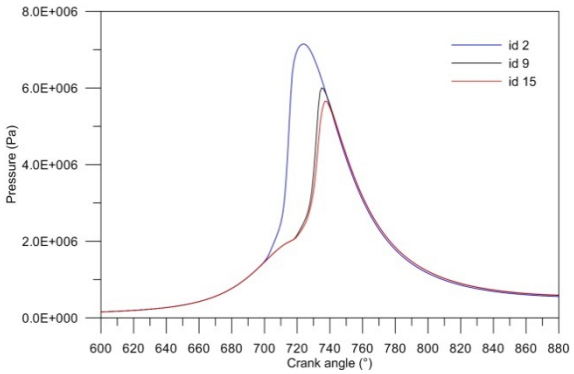

Figure 17: Computed in-cylinder pressure cycles for the three cases of Table 4.

Figure 17 represents the in-cylinder pressure cycles in the closed valve period, for the IDs of Table 4. Case indicated with ID=2 is characterised by a really high pressure gradient, as shown in Figure 17. Therefore it must be discharged. The other cases have comparable power output, but also ID=9 must be not considered due to the adopted constraint on the knocking occurrence. ID=15 is, therefore, the optimal solution, with the SOS of ID=9 (knocking condition), but a SOI occurring 130° BTDC. This shows a favourable effect of advancing injection on knocking occurrence.

7 CONCLUSIONS

Mixing control is fundamental in internal combustion engines. It assures flame stability, reduction of pollutants, improved combustion efficiency, reduced size and greater lifetimes of combustors.

Achievement of optimal charge conditions at all the engine loads and speeds in modern gasoline GDI spark ignition engines is undoubtedly a challenging task, especially if the so-called mixed mode boosting is to be realized, with homogeneous stoichiometric or rich mixtures at the higher loads, and stratified lean mixtures at the lower ones. This is the reason why fully automatic procedures to be used in the phase of definition of the engine governing parameters are strongly demanded.

Present work aims at presenting a 3D numerical model able to reproduce the in-cylinder processes of a high performance GDI engine. The model includes a sub-model for the spray dynamics tuned through an automatic procedure on the ground of an experimental campaign conducted in an optically accessible vessel, as well as a proper spray-wall impingement sub-model that accounts for the heat transferred from the wall to the liquid deposits of fuel.

The considered engine has the head of a commercial 1750 cm^3 automotive power system, but is optically accessible due to properly made modifications to the piston and engine block. This allows capturing images of both the in-cylinder mixture formation and combustion processes.

The developed 3D engine model is shown to well reproduce the in-cylinder thermo-fluidynamics under both stoichiometric and lean charges. It allows determining with very good accuracy the whole pressure cycle over the 4-stroke period, as well as the flame propagation within the combustion chamber. This highlights any inadequacy of the mixture formation process that may cause incomplete or unstable combustions.

A simplified model for the pre-flame reactions is also considered in the end-gas zone of the

combustion chamber, not yet reached by the principal flame front, in order to detect the possible occurrence of knocking through numerical simulations.

Under proper operating conditions, computations show a good agreement with experiments as regards the knocking onset and its temporal location. The spatial position being the most probable for knocking is also highlighted. The chemical reactivity in the zone not yet reached by the flame front increases as the spark advance is increased, also as a consequence of the greatest time needed for flame initiation consequent the lower in-chamber value of temperature and pressure at spark timing.

According to the performed analysis, a criterion is established to individuate the knocking occurrence from the pressure cycle trend.

The developed model is finally included within an optimization problem aimed at maximizing the engine power output by proper choice of the injection strategy and the time of spark ignition with the avoidance of knocking.

The described simulation approach may be employed in the phase of engine design to reduce the time-to-market of new technologies. If reliable experimental data available for engines of analogous configurations for validation are missing, the proposed approach may even furnish qualitative information useful for the development of control strategies.

REFERENCES

Alkidas, A. C., 2007. Combustion advancements in gasoline engines, *Energy Conversion and Management*, Vol. 48, pp. 2751–2761.

Allocca, L., Costa, M., Montanaro, A., Sementa, P., Sorge, U., Vaglieco, B.M., 2012. Characterization of the Mixture Formation Process in a GDI Engine Operating in Stratified Mode, 12th Triennial Int. Conf. on Liquid Atomization and Spray Systems, Heidelberg.

Carling, R. W., 2010. Predictive Simulation of Combustion Engine Performance in an Evolving Fuel Environment, Sandia National Laboratories.

Colin, O., Benkenida, A., Angelberger, C., 2003. 3D Modeling of Mixing, Ignition and Combustion Phenomena in Highly Stratified Gasoline Engines, *Oil & Gas Science and Technology – Rev. IFP Energies Nouvelles*, Vol. 58, pp. 47-62.

Costa, M., Sorge, U., Allocca, L., 2012. CFD optimization for GDI spray model tuning and enhancement of engine performance, *Advances in Engineering Software*, Vol. 49, pp. 43-53.

Costa, M., Marchitto, L., Merola, S.S., Sorge, U., 2014. Study of mixture formation and early flame development in a research GDI engine through numerical simulation and UV-digital imaging, *Energy,* doi: 10.1016/j.energy.2014.04.114.

Dukowicz, J.K., 1979. Quasi-steady droplet change in the presence of convection, informal report Los Alamos Scientific Laboratory, Los Alamos Report LA7997-MS.

Griffiths, J.F., Hughes, K.J., Schreiber, M., Poppe, C., Dryer, F.L., 1994. A unified approach to the reduced kinetic modeling of alkane combustion, *Combustion and Flame*, Vol. 99 (3-4), pp. 533-540.

Halstead, M.P., Kirsch, L.J., Quinn, C.P., 1977. The auto-ignition of hydrocarbon fuel at high temperatures and pressures-fitting of a mathematical model, *Combustion and Flame*, Vol. 30, pp. 45-60.

Heywood, J.B., 1988. Internal Combustion Engine Fundamentals, New York: McGraw-Hill.

Huh, K.Y., Gosman, A.D., 1991. A phenomenological model of diesel spray atomisation, International Conference on Multiphase Flows, Tsukuba, Japan.

Kuhnke, D., 2004. "Spray Wall Interaction Modeling by Dimensionless Data Analysis", PhD thesis, Technische Universität Darmstadt.

Leppard, W.R, 1991. The autoignition chemistries of octane-enhancing ethers and cyclic ethers: A motored engine study, SAE Paper 912313.

Li, H., Prabhu, S., Miller, D., Cernansky, N., 1994. Autoignition Chemistry Studies on Primary Reference Fuels in a Motored Engine, SAE Tech. Paper 942062.

Mundo, C., Sommerfeld, M., Tropea, C., 1995. Droplet-Wall Collisions: Experimental Studies of the Deformation and Breakup Process, *International Journal of Multiphase Flows*, Vol. 21(2), pp. 151-173.

Nelder, J. A., Mead, R., 1965. A simplex method for function minimization, *Computer Journal*, Vol. 7, pp. 308–313.

Nordin, W.H., 2001. Complex Modeling of Diesel Spray Combustion, Thesis (PhD), Chalmers University of Technology.

Oh H. C., Bae C. S., 2013. Effects of the injection timing on spray and combustion characteristics in a spray-guided DISI engine under lean-stratified operation, *Fuel*, Vol. 107, pp. 225–235.

O'Rourke, P.J., Bracco, F.V., 1980. Modeling of Drop Interactions in Thick Sprays and a Comparison with Experiments, IMECHE, London.

Park, C. Kim, S., Kim, H. Moriyoshi, Y., 2012. Stratified lean combustion characteristics of a spray-guided combustion system in a gasoline direct injection engine, *Energy*, Vol. 41, pp. 401-407.

Ramos, J. I., 1989. *Internal Combustion Engine Modelling*, CRC Press.

Stan, C., 2000. *Direct injection systems for spark-ignition and compression-ignition engines*, SAE Publication.

Shi, Y., Ge, H. W., Reitz, R. D., 2011. *Computational Optimization of Internal Combustion Engines*, Springer-Verlag. London.

Thévenin, D., Janiga, G. (Eds.), 2008. *Optimization and Computational Fluid Dynamics*, Springer-Verlag. Berlin Heidelberg.

Zeldovich, Y.B., Sadovnikov, P.Y., Frank-Kamenetskii, D.A., 1947. Oxidation of Nitrogen in Combustion, Translation by M. Shelef, Academy of Sciences of USSR, Institute of Chemical Physics, Moscow-Leningrad.

Zhao, H., Ladommatos, N., 2001. *Engine Combustion Instrumentation and Diagnostics*, SAE Int. Inc..